

UCSF

UC San Francisco Previously Published Works

Title

Striatal Cholinergic Interneurons Drive GABA Release from Dopamine Terminals

Permalink

<https://escholarship.org/uc/item/4w53v5p7>

Journal

Neuron, 82(1)

ISSN

0896-6273

Authors

Nelson, Alexandra B
Hammack, Nora
Yang, Cindy F
[et al.](#)

Publication Date

2014-04-01

DOI

10.1016/j.neuron.2014.01.023

Peer reviewed

Published in final edited form as:

Neuron. 2014 April 2; 82(1): 63–70. doi:10.1016/j.neuron.2014.01.023.

Striatal cholinergic interneurons drive GABA release from dopamine terminals

Alexandra B. Nelson^{1,2}, Nora Hammack¹, Cindy F. Yang³, Nirao M. Shah³, Rebecca P. Seal⁴, and Anatol C. Kreitzer^{1,2,5,*}

¹The Gladstone Institutes, San Francisco, CA, 94158

²Department of Neurology, University of California, San Francisco, CA 94158

³Department of Anatomy, University of California, San Francisco, CA 94158

⁴Department of Neurobiology, University of Pittsburgh School of Medicine, Pittsburgh, PA 15213

⁵Department of Physiology, University of California, San Francisco, CA 94158

Summary

Striatal cholinergic interneurons are implicated in motor control, associative plasticity, and reward-dependent learning. Synchronous activation of cholinergic interneurons triggers large inhibitory synaptic currents in dorsal striatal projection neurons, providing one potential substrate for control of striatal output, but the mechanism for these GABAergic currents is not fully understood. Using optogenetics and whole-cell recordings in brain slices, we find that a large component of these inhibitory responses derive from action-potential-independent disynaptic neurotransmission mediated by nicotinic receptors. Cholinergically-driven IPSCs were not affected by ablation of striatal fast-spiking interneurons, but were greatly reduced after acute treatment with vesicular monoamine transport inhibitors or selective destruction of dopamine terminals with 6-hydroxydopamine, indicating that GABA release originated from dopamine terminals. These results delineate a mechanism in which striatal cholinergic interneurons can co-opt dopamine terminals to drive GABA release and rapidly inhibit striatal output neurons.

Introduction

While they represent a sparse population of neurons within the striatum (1–2%), cholinergic interneurons have been implicated in multiple striatal functions, including motor control, associative learning, and reward (Exley and Cragg, 2008; Shuen et al., 2008). Tonically-active neurons (TANs), thought to be striatal cholinergic interneurons (Wilson et al., 1990), show precise patterns of firing during reward-based learning paradigms, suggesting a prominent role in plasticity (Cachope et al., 2012; Hanley and Bolam, 1997; Shen et al., 2005; Stuber et al., 2010). Although the precise mechanism by which cholinergic interneurons control striatal output has not yet been elucidated, recent studies provide interesting clues.

© 2014 Elsevier Inc. All rights reserved.

*corresponding author: Anatol Kreitzer, The Gladstone Institutes, 1650 Owens St, San Francisco, CA, akreitzer@gladstone.ucsf.edu.

Publisher's Disclaimer: This is a PDF file of an unedited manuscript that has been accepted for publication. As a service to our customers we are providing this early version of the manuscript. The manuscript will undergo copyediting, typesetting, and review of the resulting proof before it is published in its final citable form. Please note that during the production process errors may be discovered which could affect the content, and all legal disclaimers that apply to the journal pertain.

Activation of dorsal striatal cholinergic interneurons drives inhibitory responses in the principal cells of the striatum, medium spiny neurons (MSNs) (English et al., 2011; Sullivan et al., 2008; Witten et al., 2010). Optogenetically-evoked inhibitory postsynaptic currents (IPSCs) have two distinct components: a fast component (fIPSC) with a decay time constant of approximately 5 milliseconds (msec), and a slower component (sIPSC) with a time constant of about 90 msec (English et al., 2011). Disynaptic inhibition via a rare striatal GABAergic interneuron subtype, neurogliaform cells, appears to explain a substantial portion of the sIPSC (English et al., 2011). However, the source of the fIPSC has not been identified.

In principle, the fIPSC may be monosynaptic or disynaptic. A disynaptic process would involve first a cholinergic synapse and then a GABAergic synapse. If disynaptic, two features of the fIPSC are as yet unclear: (1) whether cholinergic control of GABA release is mediated by axon-to-dendrite versus axon-to-axon-terminal neurotransmission, and (2) what cell type releases GABA. Two cell types are good candidates by virtue of being activated by nicotinic receptors and their ability to drive large, fast inhibitory responses in MSNs: fast spiking interneurons (FSI) (Koos and Tepper, 2002) and nigrostriatal dopaminergic neurons (Cachope et al., 2012; Exley and Cragg, 2008; Threlfell et al., 2012; Zhou et al., 2001). Recent experiments have also demonstrated that dopaminergic neurons can release both dopamine and GABA, both of which depend on the vesicular monoamine transporter (VMAT) (Tritsch et al., 2012).

Here, we test the potential roles of striatal FSIs and dopamine terminals in mediating cholinergically-triggered disynaptic IPSCs in MSNs. Using a combination of methods, we demonstrate that the fast portion of the IPSC is mediated by cholinergic activation of GABA release from striatal dopaminergic terminals, which is action potential independent. These findings suggest that cholinergic interneurons are able to rapidly regulate striatal output through GABAergic inhibition, while simultaneously exerting neuromodulatory control via dopamine and acetylcholine signaling.

Results

We used an optogenetic approach to explore how cholinergic interneuron activity influences striatal output neurons. Injection of a Cre-dependent virus (AAV2/1-DIO-ChR2-mCherry) encoding channelrhodopsin-2 (ChR2) in the dorsal striatum of choline acetyltransferase (ChAT)-Cre mice produced selective ChR2 expression in striatal cholinergic interneurons (Figure 1A).

To physiologically confirm ChR2 expression in cholinergic interneurons, we performed whole-cell current-clamp recordings of mCherry-positive neurons. These neurons showed typical intrinsic properties, including spontaneous action potential firing, pronounced action potential after hyperpolarization, and a characteristic voltage sag with hyperpolarizing current (Kawaguchi, 1993) (Figure 1B). Brief (5 msec) blue light pulses triggered action potentials in mCherry-positive putative cholinergic neurons (Figure 1B).

To isolate inhibitory synaptic currents triggered by activation of cholinergic neurons, we performed whole-cell voltage-clamp recordings of medium spiny neurons in the presence of glutamate receptor antagonists NBQX and D-APV. Using a high-chloride internal solution to promote detection of GABAergic currents, blue light pulses elicited inhibitory postsynaptic currents (IPSCs) measuring 1830 ± 290 pA ($n=37$). This light-evoked IPSC was characterized by distinct phases of decay, as has been described previously (English et al., 2011): the fast phase (fIPSC) had a decay time constant of 5.2 ± 1.0 msec, while a slower phase (sIPSC) had a decay time constant of 90 ± 7 msec (Figure 1C). Both IPSC

phases were blocked by the GABA_A antagonist picrotoxin (50 μ M; 98 \pm 0.4 % block; n=6; p=0.009; Figure 1C), which was shown previously with bicuculline (English et al., 2011), confirming the IPSC is GABAergic. Delivery of two blue light pulses at short intervals produced IPSCs with marked paired-pulse depression; full recovery of the IPSC occurred between 30 and 60 seconds (Figure S1). Single blue light pulses could block action potentials in MSNs under physiological conditions (see example, Figure 1C), demonstrating the potential functional relevance of these inhibitory responses. To determine whether light-evoked IPSCs differed between direct- and indirect-pathway medium spiny neurons, a subset of experiments were performed in ChAT-Cre:Drd1a-Tomato mice, which express the fluorescent reporter tdTomato in dopamine D1 receptor-containing neurons (Shuen et al., 2008). Optogenetically-evoked IPSCs were comparable in interleaved D1-Tomato positive and negative MSNs (Figure 1D), measuring 990 \pm 210 pA (n=14) and 920 \pm 110 pA (n=12, p=0.6), respectively. To determine whether rebound firing by cholinergic interneurons could also drive IPSCs, the inhibitory opsin halorhodopsin (eNpHR3.0) was expressed in cholinergic interneurons. In ChAT-Cre mice injected with AAV5-DIO-eNpHR3.0-YFP, yellow light caused hyperpolarization of the membrane potential in cholinergic interneurons, and at the offset of such pulses, rebound spiking (Figure 1E). Voltage-clamp recordings of MSNs showed large IPSCs at the offset of yellow light pulses (Figure 1E), which were similar in amplitude (1130 \pm 230 pA; n=5) and kinetics (tau decay times for fast and slow components 6.2 \pm 1.5 and 127.6 \pm 28.2 msec, respectively) to IPSCs elicited with ChR2 activation. These findings suggest that cholinergic interneuron activity, triggered by direct depolarization or rebound following hyperpolarization, can lead to large IPSCs in MSNs.

Light-evoked IPSCs could, in principle, be derived from monosynaptic GABA release by cholinergic interneurons themselves, as has been shown in the retina (Campbell et al., 1991), or through a disynaptic mechanism (Figure S2). A disynaptic mechanism should depend on transmitter release from cholinergic interneurons onto a second class of GABA-containing neurons. Indeed, the fast portion of the IPSC was reconstituted by local application of the cholinergic agonist carbachol (10 mM) near the recorded MSN. Carbachol produced large amplitude IPSCs (850 \pm 160 pA, n=11), which were blocked by picrotoxin (50 μ M; Figure 2A). This carbachol-triggered IPSC had a tau decay of 7.2 \pm 1.1 msec (n=11) comparable to the fast component of the light-evoked IPSC, suggesting that local application could selectively recruit GABA release responsible for the fIPSC. Carbachol-triggered IPSCs were also blocked by the nicotinic antagonist mecamylamine (5 μ M, Figure 2A), indicating that they are mediated by nicotinic acetylcholine receptors. Dependence of light-evoked responses on acetylcholine release was confirmed using cholinergic receptor antagonists. IPSC amplitude was not significantly reduced by the muscarinic antagonist scopolamine (10 μ M; 3 \pm 7% block; n=5; p=0.39) or the α 7 nicotinic receptor antagonist methyllycaonitine (MLA, 10 nM; 15 \pm 11% block; n=7; p=0.14), but was potently inhibited by the nicotinic antagonists mecamylamine (5 μ M; 92 \pm 7% block; n=5; p=0.038) and dihydrobetaerythroidine (DH β E, 10 μ M; 93 \pm 3% block; n=5; p=0.034; Figure 2B). These experiments demonstrated that the IPSC depends on non- α 7-containing nicotinic acetylcholine receptors, and suggested a disynaptic mechanism.

Disynaptic IPSCs could derive from cholinergic stimulation of an action potential in a second neuron, resulting in action-potential-dependent release of GABA onto MSNs. Alternatively, acetylcholine could activate nicotinic receptors at sites of GABA release, eliciting IPSCs in MSNs without a requirement for action potentials (see Figure S2). To investigate this latter possibility, we activated cholinergic interneurons and recorded IPSCs in MSNs while applying the sodium channel antagonist tetrodotoxin (TTX, 1 μ M), which would be expected to block action potentials in both the cholinergic interneuron and putative GABAergic neurons. TTX application resulted in a complete block of the disynaptic IPSC

(Figure 2C). However, application of TTX together with the potassium channel antagonist 4-aminopyridine (4-AP, 100 μ M), which enables ChR2-mediated release of neurotransmitter without action potentials (Petreanu et al., 2012), partially restored the IPSC (Figure 2C). The average amplitude of IPSCs after addition of TTX and 4-AP was 43 \pm 11% (n=14) of the control IPSC, and the area under the IPSC (net charge) after addition of TTX and 4-AP was 77 \pm 17% of the control IPSC (n=14, Figure 2C). Using a similar method, the net charge of the carbachol-triggered IPSC in the presence of TTX and 4-AP was 79 \pm 16% of control (n=6, Figure 2C). These results support the hypothesis that a substantial portion of the IPSC triggered by cholinergic interneuron stimulation is through an action-potential-independent mechanism.

Though activation of nicotinic receptors led to GABA release, it was unclear whether synaptic vesicle release was triggered directly by calcium influx through nicotinic receptors or through recruitment of additional calcium sources, such as voltage-gated calcium channels or internal calcium stores. As optogenetically-evoked IPSCs were blocked by DH β E but not by MLA, the nicotinic receptors involved are a non- α 7-containing subtype, with lower calcium permeability (Rice and Cragg, 2004), and are thus less likely to participate directly in vesicle fusion. Suspecting voltage-gated calcium channels might provide the necessary calcium, we elicited IPSCs with pressure-ejected carbachol, and applied cadmium chloride, a nonselective blocker of voltage-gated calcium channels that does not block α 4-containing nicotinic receptors (Karadsheh et al., 2004). Cadmium markedly reduced IPSC amplitude (n=5; p=0.01; Figure 2D), suggesting voltage-gated calcium channels are required for nicotinic activation of GABA release. In the hippocampus, nicotinic depolarization of axon terminals triggers GABA release through T-type calcium channels (Tang et al., 2011), so we proceeded to test the role of these channels in light-evoked disynaptic inhibition. The specific T-type calcium channel blocker mibefradil (5 μ M) reduced the light-evoked IPSC by 41 \pm 6% (n=8, p=0.02; data not shown) and the carbachol-evoked IPSC by 67 \pm 3% (n=4, Figure 2D). Together, these results suggest that presynaptic nicotinic receptor activation leads to the recruitment of voltage-gated calcium channels, including T-type channels, to cause sufficient calcium influx for release of GABA onto MSNs.

While these findings suggest that the fIPSC triggered by activation of cholinergic interneurons is likely to be disynaptic and action-potential-independent, they do not indicate which neurons release GABA. Fast-spiking interneurons (FSI) drive large inhibitory synaptic responses in MSNs, making them a candidate source of GABA for the fast disynaptic IPSC (Gittis et al., 2010; Koos and Tepper, 1999). To determine whether FSI are required for disynaptic inhibition, we selectively ablated a majority of the parvalbumin (PV)-positive FSIs by injecting the striatum of PV-Cre mice (Figure 3A) with a Cre-dependent virus encoding pro-Caspase3 and an enzyme that cleaves pro-Caspase3 into the active, pro-apoptotic signal Caspase3 (Yang et al., 2013). PV-positive cells were greatly diminished in the AAV-FLEX-taCasp3-TEVp-injected striatum as compared to the contralateral control striatum (3 \pm 1 vs 56 \pm 6 PV-positive dorsal striatal neurons per section; N= 7 mice; Figure 3B, C). As a positive control that this manipulation could eliminate monosynaptic inhibition from FSI onto MSN, we injected PV-Cre mice with bilateral AAV1-DIO-ChR2-YFP and unilateral AAV1-FLEX-taCasp3-TEVp. Slices contralateral to AAV1-FLEX-taCasp3-TEVp injection showed expression of ChR2-YFP in PV-positive putative FSI (Figure S3B), while in ipsilateral slices very few PV positive neurons were detected, (Figures 3B,C, S3A); most of these remaining neurons expressed ChR2-YFP. Presumed monosynaptic FSI-mediated IPSCs were large in control slices (5880 \pm 530 pA; n=7), but negligible in caspase-treated slices (30 \pm 8 pA; n=13, N=3 mice; p=0.0001; Figure 3C), demonstrating that near-complete elimination of PV neurons resulted in near-complete loss of the FSI-mediated IPSC in MSNs. To determine whether elimination

of PV-positive neurons and their input onto MSNs would likewise reduce the disynaptic IPSC derived from activation of cholinergic interneurons, we injected AAV1-FLEX-taCasp3-TEVp unilaterally in ChAT-ChR2::PV-Cre mice. In these mice, ChR2 is expressed constitutively in cholinergic interneurons (Zhao et al., 2011). Interestingly, ablation of PV-positive neurons (Figure 3B,D) did not significantly alter light-evoked disynaptic IPSCs (1110 \pm 370 pA; n=18 neurons/N=4 mice in the injected hemisphere versus 960 \pm 340 pA; n=13 neurons/N=4 mice in the untreated hemisphere; p=0.79; Figure 3D). These results demonstrate that FSIs are not required for disynaptic IPSCs and suggest the majority of the fIPSC is derived from an alternate source of GABA.

Given that (1) optogenetic activation of cholinergic interneurons can drive terminal dopamine release in the striatum (Cachope et al., 2012; Threlfell et al., 2012), and (2) anatomical studies (Campbell et al., 1991; Gonzalez-Hernandez et al., 2001) and a recent physiological study (Tritsch et al., 2012) suggest striatal dopaminergic axon terminals may release GABA, we hypothesized that the fIPSC was derived from cholinergic activation of dopaminergic axon terminals, resulting in GABA release. To test this hypothesis, we compared disynaptic IPSCs in slices from animals treated unilaterally with saline (control) or the dopaminergic neurotoxin 6-hydroxydopamine (6-OHDA). Degeneration of dopaminergic axons ipsilateral to the injection was confirmed by post-hoc tyrosine hydroxylase staining (Figure 4A). 6-OHDA treatment resulted in markedly reduced light-evoked IPSCs (170 \pm 40 pA, n=14 neurons/N=4 mice) as compared to saline treatment (Figure 4B, C; 1610 \pm 410 pA, n=10 neurons/N=3 mice, p=0.0006). This result suggests that the fIPSC triggered by activation of cholinergic interneurons depends on the integrity of nigrostriatal dopamine neurons. To further investigate whether depletion of neurotransmitter from dopamine terminals alters IPSC amplitude, we compared disynaptic IPSCs in slices from mice treated with the VMAT inhibitor reserpine and interleaved control mice. Although a provocative finding, a prior study showed that inhibition of VMAT prevented dopamine and GABA release from striatal dopamine terminals (Tritsch et al., 2012). We found markedly reduced IPSC amplitudes in reserpine-treated mice (240 \pm 40 pA, n=19; N=3 mice) compared to interleaved control mice (Figure 4B, C; 1760 \pm 90 pA, n=14; N=5 mice; p=0.0001), indicating that IPSCs depend on VMAT. Surprisingly, 6-OHDA and reserpine treatment resulted in reductions of both fast and slow IPSC components: neuropeptide Y-expressing neurogliaform (NPY-NGF) neurons contribute prominently to the sIPSC (English et al., 2011). Suspecting that the chronicity of 6-OHDA and reserpine treatment might lead to striatal microcircuit reorganization and downregulation of the NPY-NGF-mediated sIPSC, we next used the more rapid-acting VMAT inhibitors Ro4-1284 and tetrabenazine (TBZ). These two agents were administered either in vivo immediately before slicing (Ro4-1284) or ex vivo to slices (TBZ). Acute Ro4-1284 treatment also reduced the amplitude of disynaptic IPSCs (670 \pm 170 pA; n=13 neurons/N=2 mice) as compared to Ro4-1284 treatment followed by ACSF wash for at least one hour (Figure 4B, C; 1840 \pm 360 pA; n=12 neurons/N=2 mice; p=0.006), but left a substantial residual sIPSC. TBZ treatment decreased IPSC amplitude (740 \pm 130 pA; n=7 neurons/N=3 mice) compared to interleaved controls (Figure 4B, C; 2570 \pm 770 pA; n=9 neurons/N=3 mice; p=0.04), also leaving a residual sIPSC (decay tau 152 \pm 26 msec). To verify that the decreased amplitude of IPSCs was not due to loss of dopamine-mediated neuromodulation of the IPSC itself, a cocktail of D1 and D2 dopamine receptor antagonists (SCH23390, 1 μ M; sulpiride, 10 μ M) was applied to control slices. Dopamine antagonists did not significantly alter IPSC amplitude (Figure 4B; 94 \pm 8% of control, n=6; p=0.54). Together, these findings strongly suggest that dopaminergic terminals provide a major source of the GABA underlying fast disynaptic IPSCs seen in MSNs following stimulation of cholinergic interneurons.

Discussion

We have demonstrated that optogenetic activation of striatal cholinergic neurons triggers a disynaptic inhibitory synaptic response in MSNs, mediated in large part by nicotinic activation of GABA release from dopamine terminals. Surprisingly, parvalbumin-positive FSI, a major source of GABAergic inputs to MSNs, are not required. As this phenomenon is TTX-insensitive, and axons are the only portion of dopamine neurons present in our preparation, acetylcholine appears to trigger striatal GABA release via an action-potential-independent axo-axonic mechanism. These findings link prior studies showing (1) inhibitory responses in MSNs driven by optogenetic activation of striatal cholinergic interneurons, (2) inhibitory responses in MSNs driven by optogenetic activation of striatal dopamine terminals, and (3) dopamine release driven by optogenetic activation of striatal cholinergic interneurons, and provide a mechanism by which striatal cholinergic interneurons may potentially influence striatal output by dual control of dopamine and GABA release.

One potential caveat of our study and others using BAC transgenic animals for optical control of cholinergic neurons is that ChAT-ChR2 mice have recently been found to have elevated ACh release and cognitive deficits due to overexpression of vesicular ACh transporters (Kolisnyk et al., 2013). Increased ACh release may enhance the amplitude of ACh-dependent responses, but is unlikely to alter the overall mechanisms we have outlined.

The finding that fast GABAergic currents in MSNs derive from dopamine terminals is intriguing. Though dopamine axon terminals do not always form traditional tight axo-dendritic synapses onto MSNs (Descarries et al., 1996), they do form a relatively uniform and dense lattice of inputs in the dorsal striatum (Hanley and Bolam, 1997), and dopamine may influence postsynaptic targets over a broad area encompassing tens of thousands of synapses (Rice and Cragg, 2008). Terminal GABA release may also operate via volume-transmission or alternatively, the IPSCs we observe may arise from GABA release at dopamine terminals that are located proximal to GABAergic synapses.

Optogenetics provides a tool for synchronous selective activation of striatal cholinergic interneurons, but prior anatomical and physiological studies have outlined much of the signaling substrate. Nicotinic acetylcholine receptors reside on dopaminergic axon terminals (Jones et al., 2001; Threlfell et al., 2010), providing the anatomical means for acetylcholine to drive the release of dopamine (and GABA) from axon terminals in the striatum. In addition, the regulation of dopamine release by nicotinic receptors has been demonstrated directly (Rice and Cragg, 2004; Zhang and Sulzer, 2004; Zhou et al., 2001). These studies have shown that while phasic cholinergic stimulation can cause dopamine release, more prolonged stimulation results in nicotinic receptor desensitization and reduced release, which may be responsible for many of the behavioral pharmacology results obtained with nicotinic agents *in vivo*. By allowing precisely timed, synchronous release of acetylcholine and subsequent stimulation of nicotinic receptors, optogenetic strategies have facilitated detecting phasic responses in the striatum, which appear to be opposite in polarity to those seen with more tonic manipulations of acetylcholine.

Despite evidence that cholinergic signaling is critical for striatal behaviors, how cholinergic interneurons alter striatal output is unclear. Spontaneously firing cholinergic interneurons receive strong excitatory thalamic input, which carries cue-related information, and inhibitory inputs from midbrain GABAergic neurons (Brown et al., 2012). In many *in vivo* studies, cholinergic neurons display a burst-pause-burst pattern of firing during relevant cues in the context of learned tasks. Cholinergic neurons send their projections widely throughout the striatum, influencing most striatal neurons through muscarinic or nicotinic receptors. Nicotinic receptor activation may have distinct phasic and tonic effects on MSNs due to the

prominent desensitization of many nicotinic subtypes. The stereotyped burst-pause-burst firing pattern of cholinergic neurons could allow for (1) a window of relief from desensitization, and (2) a more concerted modulation of MSN firing by release of fast-acting GABA and longer-acting dopamine during the burst. Afterwards, spontaneous firing of cholinergic interneurons could again result in nicotinic desensitization and reduced dopamine and GABA release. These same processes may also influence the cholinergic interneurons themselves, given the proximity of dopamine terminals and cholinergic interneurons. While the significance of each of these mechanisms to the function of striatal cholinergic interneurons *in vivo* is not yet known, the ability of these neurons to recruit both dopamine and GABA release to modulate striatal output is likely to significantly contribute to their influence of basal ganglia function.

Experimental Procedures

Detailed methods are in Supplemental Experimental Procedures.

Animals

Hemizygous ChAT-Cre mice (line GM60, GENSAT) were bred against either wild-type C57Bl/6 mice (Jackson Labs) or *Drd1a*-tdTomato mice (Nicole Calakos, Duke University) to yield ChAT-Cre or ChAT-Cre:*Drd1a*-tdTomato mice. Hemizygous ChAT-ChR2 mice (Jackson Labs) were crossed to Parvalbumin-2A-Cre mice (Jackson Labs) to yield ChAT-ChR2:PV-Cre mice. Mice of either sex were used.

Surgery

Virus was stereotactically injected in the dorsal striatum of mice through a small hole in the skull. Mice returned to their home cages for 2–4 weeks prior to histology or physiology. Some mice were later re-anesthetized and injected with either the toxin 6-hydroxydopamine or normal saline in the medial forebrain bundle.

Physiology

Mice were deeply anesthetized prior to removing the brain and preparing 300 μm coronal slices. Slices were stored in carbogenated ACSF at RT, then transferred to a recording chamber superfused with carbogenated ACSF at 31–33°C. Neurons were patched in the dorsal striatum in whole-cell mode, and ChR2 or eNpHR3.0 was activated with light pulses delivered through the microscope objective. With the exception of carbachol, which was pressure-ejected from a glass pipet, drugs were administered in the circulating ACSF.

Histology

A subset of mice were deeply anesthetized, perfused and fixed. Brains were removed, cryoprotected, and frozen, and cut into 30 μm coronal sections. Primary antibody (Millipore AB144P Anti-ChAT 1:500, SWANT Anti-parvalbumin 1:1000 or Pei-Freez P40101 Anti-Tyrosine Hydroxylase 1:1000) was added in 5% NDS, 1% Triton in PBS and incubated overnight at 4°C. After washing, slices were incubated with Alexa-Fluor 649-conjugated donkey anti-goat or donkey anti-rabbit secondary antibody (Invitrogen) for two hours at room temperature (RT).

Statistics

All data are presented as the mean \pm standard error. Comparisons were made using the student's T test.

Supplementary Material

Refer to Web version on PubMed Central for supplementary material.

Acknowledgments

Funded by the A.P. Giannini Research fellowship (ABN), NINDS K08 NS081001 (ABN), NINDS R01 NS064984 and R01 NS078435 (ACK), NINDS R01 NS049488 and R01 NS083872 (NMS) and startup funds from the University of Pittsburgh (RPS). We thank Dan Gray and Jim Wells for their help in generating the FLEX-taCasp3-TEVp construct and Diane Nathaniel and Delanie Schulte for technical assistance.

References

- Brown MT, Tan KR, O'Connor EC, Nikonenko I, Muller D, Luscher C. Ventral tegmental area GABA projections pause accumbal cholinergic interneurons to enhance associative learning. *Nature*. 2012; 492:452–456. [PubMed: 23178810]
- Cachope R, Mateo Y, Mathur BN, Irving J, Wang HL, Morales M, Lovinger DM, Cheer JF. Selective activation of cholinergic interneurons enhances accumbal phasic dopamine release: setting the tone for reward processing. *Cell reports*. 2012; 2:33–41. [PubMed: 22840394]
- Campbell KJ, Takada M, Hattori T. Co-localization of tyrosine hydroxylase and glutamate decarboxylase in a subpopulation of single nigrostriatal projection neurons. *Brain research*. 1991; 558:239–244. [PubMed: 1685932]
- Descarries L, Watkins KC, Garcia S, Bosler O, Doucet G. Dual character, asynaptic and synaptic, of the dopamine innervation in adult rat neostriatum: a quantitative autoradiographic and immunocytochemical analysis. *J Comp Neurol*. 1996; 375:167–186. [PubMed: 8915824]
- English DF, Ibanez-Sandoval O, Stark E, Tecuapetla F, Buzsaki G, Deisseroth K, Tepper JM, Koos T. GABAergic circuits mediate the reinforcement-related signals of striatal cholinergic interneurons. *Nature neuroscience*. 2011; 15:123–130.
- Exley R, Cragg SJ. Presynaptic nicotinic receptors: a dynamic and diverse cholinergic filter of striatal dopamine neurotransmission. *British journal of pharmacology*. 2008; 153(Suppl 1):S283–297. [PubMed: 18037926]
- Gittis AH, Nelson AB, Thwin MT, Palop JJ, Kreitzer AC. Distinct roles of GABAergic interneurons in the regulation of striatal output pathways. *J Neurosci*. 2010; 30:2223–2234. [PubMed: 20147549]
- Gonzalez-Hernandez T, Barroso-Chinea P, Acevedo A, Salido E, Rodriguez M. Colocalization of tyrosine hydroxylase and GAD65 mRNA in mesostriatal neurons. *Eur J Neurosci*. 2001; 13:57–67. [PubMed: 11135004]
- Hanley JJ, Bolam JP. Synaptology of the nigrostriatal projection in relation to the compartmental organization of the neostriatum in the rat. *Neuroscience*. 1997; 81:353–370. [PubMed: 9300427]
- Jones IW, Bolam JP, Wonnacott S. Presynaptic localisation of the nicotinic acetylcholine receptor beta2 subunit immunoreactivity in rat nigrostriatal dopaminergic neurones. *J Comp Neurol*. 2001; 439:235–247. [PubMed: 11596051]
- Karadsheh MS, Shah MS, Tang X, Macdonald RL, Stitzel JA. Functional characterization of mouse alpha4beta2 nicotinic acetylcholine receptors stably expressed in HEK293T cells. *Journal of neurochemistry*. 2004; 91:1138–1150. [PubMed: 15569257]
- Kawaguchi Y. Physiological, morphological, and histochemical characterization of three classes of interneurons in rat neostriatum. *J Neurosci*. 1993; 13:4908–4923. [PubMed: 7693897]
- Kolisnyk B, Guzman MS, Raulic S, Fan J, Magalhaes AC, Feng G, Gros R, Prado VF, Prado MA. ChAT-ChR2-EYFP Mice Have Enhanced Motor Endurance But Show Deficits in Attention and Several Additional Cognitive Domains. *J Neurosci*. 2013; 33:10427–10438. [PubMed: 23785154]
- Koos T, Tepper JM. Inhibitory control of neostriatal projection neurons by GABAergic interneurons. *Nature neuroscience*. 1999; 2:467–472.
- Koos T, Tepper JM. Dual cholinergic control of fast-spiking interneurons in the neostriatum. *J Neurosci*. 2002; 22:529–535. [PubMed: 11784799]

- Petreaanu L, Gutnisky DA, Huber D, Xu NL, O'Connor DH, Tian L, Looger L, Svoboda K. Activity in motor-sensory projections reveals distributed coding in somatosensation. *Nature*. 2012; 489:299–303. [PubMed: 22922646]
- Rice ME, Cragg SJ. Nicotine amplifies reward-related dopamine signals in striatum. *Nature neuroscience*. 2004; 7:583–584.
- Rice ME, Cragg SJ. Dopamine spillover after quantal release: rethinking dopamine transmission in the nigrostriatal pathway. *Brain research reviews*. 2008; 58:303–313. [PubMed: 18433875]
- Shen W, Hamilton SE, Nathanson NM, Surmeier DJ. Cholinergic suppression of KCNQ channel currents enhances excitability of striatal medium spiny neurons. *J Neurosci*. 2005; 25:7449–7458. [PubMed: 16093396]
- Shuen JA, Chen M, Gloss B, Calakos N. Drd1a-tdTomato BAC transgenic mice for simultaneous visualization of medium spiny neurons in the direct and indirect pathways of the basal ganglia. *J Neurosci*. 2008; 28:2681–2685. [PubMed: 18337395]
- Stuber GD, Hnasko TS, Britt JP, Edwards RH, Bonci A. Dopaminergic terminals in the nucleus accumbens but not the dorsal striatum corelease glutamate. *J Neurosci*. 2010; 30:8229–8233. [PubMed: 20554874]
- Sullivan MA, Chen H, Morikawa H. Recurrent inhibitory network among striatal cholinergic interneurons. *J Neurosci*. 2008; 28:8682–8690. [PubMed: 18753369]
- Tang AH, Karson MA, Nagode DA, McIntosh JM, Uebele VN, Renger JJ, Klugmann M, Milner TA, Alger BE. Nerve terminal nicotinic acetylcholine receptors initiate quantal GABA release from perisomatic interneurons by activating axonal T-type (Cav3) Ca(2) channels and Ca(2) release from stores. *J Neurosci*. 2011; 31:13546–13561. [PubMed: 21940446]
- Threlfell S, Clements MA, Khodai T, Pienaar IS, Exley R, Wess J, Cragg SJ. Striatal muscarinic receptors promote activity dependence of dopamine transmission via distinct receptor subtypes on cholinergic interneurons in ventral versus dorsal striatum. *J Neurosci*. 2010; 30:3398–3408. [PubMed: 20203199]
- Threlfell S, Lalic T, Platt NJ, Jennings KA, Deisseroth K, Cragg SJ. Striatal dopamine release is triggered by synchronized activity in cholinergic interneurons. *Neuron*. 2012; 75:58–64. [PubMed: 22794260]
- Tritsch NX, Ding JB, Sabatini BL. Dopaminergic neurons inhibit striatal output through non-canonical release of GABA. *Nature*. 2012; 490:262–266. [PubMed: 23034651]
- Wilson CJ, Chang HT, Kitai ST. Firing patterns and synaptic potentials of identified giant aspiny interneurons in the rat neostriatum. *J Neurosci*. 1990; 10:508–519. [PubMed: 2303856]
- Witten IB, Lin SC, Brodsky M, Prakash R, Diester I, Anikeeva P, Gradinaru V, Ramakrishnan C, Deisseroth K. Cholinergic interneurons control local circuit activity and cocaine conditioning. *Science (New York, NY)*. 2010; 330:1677–1681.
- Yang CF, Chiang MC, Gray DC, Prabhakaran M, Alvarado M, Juntti SA, Unger EK, Wells JA, Shah NM. Sexually dimorphic neurons in the ventromedial hypothalamus govern mating in both sexes and aggression in males. *Cell*. 2013; 153:896–909. [PubMed: 23663785]
- Zhang H, Sulzer D. Frequency-dependent modulation of dopamine release by nicotine. *Nature neuroscience*. 2004; 7:581–582.
- Zhao S, Ting JT, Atallah HE, Qiu L, Tan J, Gloss B, Augustine GJ, Deisseroth K, Luo M, Graybiel AM, et al. Cell type-specific channelrhodopsin-2 transgenic mice for optogenetic dissection of neural circuitry function. *Nature methods*. 2011; 8:745–752. [PubMed: 21985008]
- Zhou FM, Liang Y, Dani JA. Endogenous nicotinic cholinergic activity regulates dopamine release in the striatum. *Nature neuroscience*. 2001; 4:1224–1229.

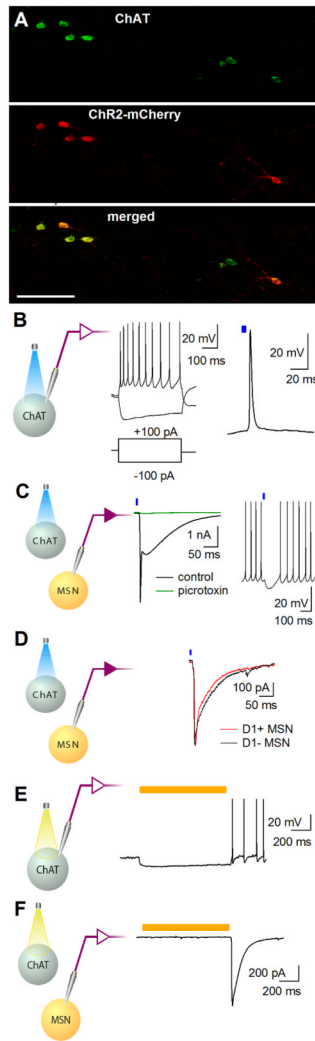


Figure 1. Optogenetic activation of striatal cholinergic interneurons elicits inhibitory synaptic responses

A–D. Dorsal striatal slices from ChAT-Cre mice injected with AAV-DIO-ChR2-mCherry. A. Immunohistochemistry for ChAT (top), mCherry (middle), and merged (bottom), showing mCherry positive neurons were positive for ChAT. Scale bar = 100 μ m. B. Left panel: recording configuration. Current clamp recording from an mCherry-positive, putative cholinergic interneuron. Membrane potential responses to injection of \pm 100 pA (middle panel) or a single 5 msec light pulse (470 nm, blue bar, right panel). C. Left panel: recording configuration. Middle panel: Voltage-clamp recording from a medium spiny neuron (MSN). Blue light pulses evoked a large inward current with two phases before (black) and after (green) application of picROTOXIN (50 μ M). Right panel: current-clamp recording from an MSN depolarized to fire action potentials. A blue light pulse caused a brief pause in the firing of the MSN. D. Left panel: recording configuration. Right panel: synaptic currents from a D1-Tomato positive MSN (red trace) and a nearby D1-Tomato negative MSN (black trace) in response to blue light pulses. E, F. Recordings made in ChAT-Cre mice injected with AAV-DIO-eNpHR3.0-YFP. E. Left panel: recording configuration. Right panel: current-clamp recording from a YFP-positive, putative cholinergic interneuron, showing hyperpolarization followed by rebound firing in response to a 1000 msec light pulse (554

nm, yellow bar). F. Left panel: recording configuration. Right panel: a large IPSC in an MSN at the offset of the light pulse.

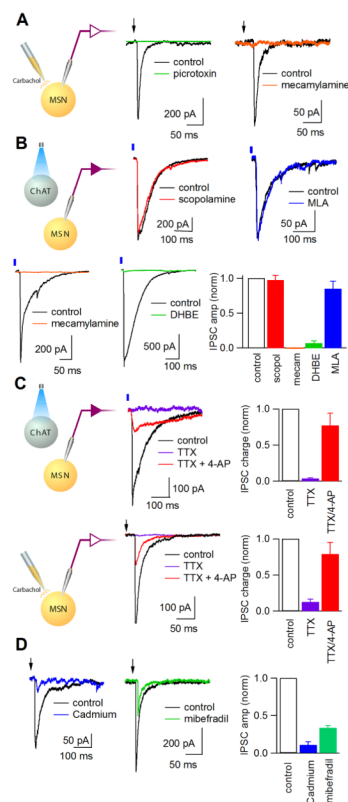


Figure 2. Disynaptic inhibitory synaptic responses are action potential independent

A. Voltage-clamp recording from an MSN, showing the inward current triggered by carbachol (10 mM), locally pressure-ejected from a pipet positioned nearby (schematic at left). The carbachol-evoked current is shown before (black) and after (green) bath application of picrotoxin (50 μ M; middle panel) and before (black) and after (orange) bath application of the nicotinic antagonist mecamylamine (5 μ M; right panel). B. Representative light-evoked inhibitory synaptic responses (schematic at left) before (black) and after application of the muscarinic antagonist scopolamine (10 μ M, red), the nicotinic antagonists mecamylamine (5 μ M, orange) and dihydrobetaerythroidine (DH β E, 10 μ M, green), and the α 7 nicotinic antagonist methyllycaconitine (MLA, 10 nM, blue). Right panel: Normalized IPSC amplitude. C. Upper panels: Light-activated IPSCs in MSNs (schematic at left). The disynaptic IPSC (black) was abolished by bath application of tetrodotoxin (TTX, 1 μ M, purple) then partly restored by TTX + 4-aminopyridine (4-AP; 100 μ M, red). Right panel: Normalized net IPSC charge. Lower panels: Carbachol-evoked IPSCs in MSNs (schematic at left) at baseline (black) and after TTX (purple) and TTX + 4-AP (red). Right panel: Normalized net IPSC charge. D. Carbachol-evoked IPSCs in MSNs at baseline (black trace) and after application of cadmium chloride (100 μ M; left panel, blue trace) or mibefradil (100 μ M; middle panel, green trace). Right panel: Normalized IPSC amplitude. All bars mean \pm SEM.

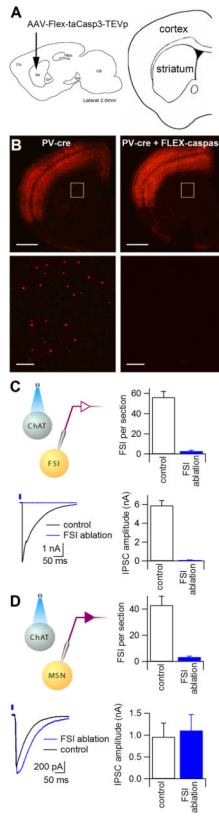


Figure 3. Ablation of parvalbumin-positive fast-spiking interneurons does not alter the disynaptic IPSC

The dorsolateral striatum of PV-Cre mice was injected with AAV1-FLEX-taCasp3-TEVp to ablate parvalbumin (PV)-positive neurons. A. Upper panels: diagrams of the brain in sagittal view (left), showing the area of viral injection, and coronal view (right), showing the structures in histological sections below. B. Coronal sections immunostained for PV (red). Upper panels: Control (uninjected) hemisphere (left) and hemisphere injected with AAV1-FLEX-taCasp3-TEVp (right). Scale bar = 1 mm. Inset: area of dorsal striatum where physiological recordings were made. Lower panels: Control (uninjected, left) and FSI-ablation (injected, right) sections, showing striatal PV-positive neurons. Scale bar = 150 μ m. C. Recordings made from PV-Cre mice injected with bilateral AAV1-DIO-ChR2-YFP and unilateral AAV1-FLEX-taCasp3-TEVp. Upper left: recording configuration. Upper right: average number of PV-positive neurons per hemisphere of the dorsal striatum in control (ChR2 only) and FSI ablation (ChR2 + caspase) conditions. Lower left: Representative light-activated (presumed monosynaptic) currents elicited in MSNs in the control (black) and FSI ablation (blue) conditions. Lower right: average IPSC amplitude in control versus FSI ablation slices. D. Recordings made from PV-Cre:ChAT-ChR2 mice injected with unilateral AAV-FLEX-taCasp3-TEVp. Upper left: recording configuration. Upper right: average number of PV-positive neurons per hemisphere of the dorsal striatum in control and FSI ablation conditions. Bottom left: Representative light-activated (presumed disynaptic) currents in MSNs in control (black) and FSI ablation (blue) conditions. IPSCs recorded at -70 mV in the presence of NBQX and APV. Lower right: average IPSC amplitude in control versus FSI ablation slices. All bars represent mean \pm SEM.

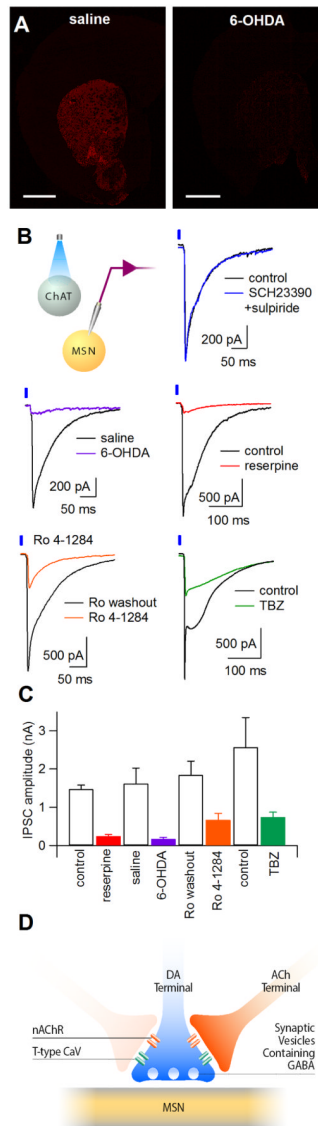


Figure 4. Disynaptic inhibitory responses require dopaminergic neurons

A. Coronal sections containing the striatum immunostained for tyrosine hydroxylase (red). Left panel: striatum of mouse injected with saline. Right panel: striatum of mouse injected with 6-OHDA. Scale bar = 1 mm. B. Recording configuration. Representative light-evoked currents in MSNs from ChAT-Cre animals injected with striatal AAV-DIO-ChR2-mCherry. IPSCs are shown at baseline (black) versus after 10 minutes application of SCH23390 (1 μ M) and sulpiride (10 μ M, blue); in slices from saline-injected (black) versus 6-OHDA-injected (purple) mice; interleaved control (black) versus reserpine-injected (red) mice; Ro4-1284-incubated (orange) versus Ro4-1284 washout (black) slices from the same Ro4-1284-injected mice; tetrabenazine-treated (green) versus interleaved control (black) mice. C. Summary of light-evoked IPSCs. D. Schematic diagram of proposed microcircuit involving striatal cholinergic interneurons (red), nigrostriatal dopamine terminals (blue) and medium spiny neuron dendrites (yellow). All bars represent mean \pm SEM.